applied sciences

MDPI

Article

Stereotactic Positioning System: Towards a Mechanism Used in Thermal Ablation Therapy

Jose Mendez Maria [1], Gemima Lara Hernandez [1], Citlalli Jessica Trujillo-Romero [2,*], Albino Martinez Sibaja [1] and Jose Jesus Agustín Flores Cuautle [3,*]

[1] TecNM, Instituto Tecnológico de Orizaba, Orizaba 94320, Mexico; josemendezmaria@gmail.com (J.M.M.); larag_139@hotmail.com (G.L.H.); albino.ms@orizaba.tecnm.mx (A.M.S.)
[2] Division de Investigación en Ingeniería Médica, Instituto Nacional de Rehabilitación-LGII, Mexico City 14389, Mexico
[3] Consejo Nacional de Ciencia y Tecnologia, Tecnológico Nacional de México, Instituto Tecnológico de Orizaba, Orizaba 94320, Mexico
* Correspondence: cjtrujillo@inr.gob.mx (C.J.T.-R.); jflores_cuautle@hotmail.com (J.J.A.F.C.)

Abstract: In microwave thermal ablation, placing the antenna on a specific coordinate is one of the most critical steps. Several stereotactic systems can place an instrument on a specific point with great accuracy. However, these systems are developed for neurosurgery; moreover, a stereotactic system used in microwave thermal ablation must not disturb the electromagnetic (EM) pattern generated by the antenna. A stereotactic positioning system was designed, built, and tested. Different types of materials were proposed to manufacture the proposed stereotactic system to locate the microwave antennas. The stereotactic system can displace the microwave antenna around the Z-axis and Theta-axis. Displacements were generated by stepper motors and controlled by the user through a graphical interface. The system tests consist of programming displacements along the two axes in steps of 5 mm on the Z-axis and 5 degrees on the Theta-axis. Results showed that the system is capable of moving using cylindrical coordinates over a 70 mm displacement with an average error of ±0.85 mm for sensors on the Z-axis, while in the Theta-axis it reaches 180° displacement with an error of ±2.64°. A stereotactic microwave antenna positioning system was developed and preliminarily tested. This first system can already be used to evaluate antenna performance either in phantoms or ex-vivo tissue. Moreover, this system can be extrapolated to different parts of the human body and be adapted to the required dimensions.

Keywords: thermal ablation; microwave antenna; leg stereotactic systems; electromechanical device

Citation: Mendez Maria, J.; Lara Hernandez, G.; Trujillo-Romero, C.J.; Martinez Sibaja, A.; Flores Cuautle, J.J.A. Stereotactic Positioning System: Towards a Mechanism Used in Thermal Ablation Therapy. *Appl. Sci.* **2022**, *12*, 7795. https://doi.org/10.3390/app12157795

Academic Editor: Nicola Pio Belfiore and Fabio Di Pietrantonio

Received: 31 May 2022
Accepted: 30 July 2022
Published: 3 August 2022

1. Introduction

Stereotactic systems are devices used to place surgical instruments in two-dimensional and three-dimensional space. These systems have been developed for neurosurgery because they can place or maintain instruments on a specific point or target with excellent stability and accuracy. Commercial stereotactic systems such as Leksell [1] and Brown-Roberts-Wells (BRW) [2] were developed for neurosurgery applications. These systems are generally composed of the following components [3]: (1) stereotactic frame, (2) helmet, locators, or reference systems, (3) stereotactic guide that can slide over the frame, (4) instrumentation, and (5) planning systems.

The applications that require the use of stereotactic systems are procedures where great accuracy is required, e.g., brain biopsies, brain tumors treatment [4], placement of catheters for cyst drainage, placement of electrodes for deep brain stimulation (DBS) [5], and stereotactic aspirations for intracerebral hemorrhage [6]. Nowadays, new applications for stereotactic systems have been found either in radiotherapy [7] or in radiosurgery [8,9] to implement tumor treatments in different body parts [10].

Thermal ablation treatment is one of these potential new areas of application. Thermal ablation can be applied by using radiofrequency, microwave, and ultrasound. Microwave

Thermal Ablation (MTA) refers to a temperature increase of around 60–100 °C at a specific point in the body (tumor) for a particular time. Therefore, the cancer cells either burn or alter their genetic composition, stopping their excessive reproduction [11]. MTA is considered a minimally invasive treatment because the micro-coaxial antennas can be located at a specific point over the tumor utilizing a small percutaneous incision. Ultrasound or computerized tomography are used to guide the antenna inside the tumor. The micro-coaxial antenna generates an electromagnetic field that interacts with the tumor and the healthy tissue. One of the main advantages of thermal ablation to treat cancer is the generation of fewer side effects; moreover, they are more tolerable than those generated by chemotherapy or surgery [10]. The temperature distribution generated by the micro-coaxial antenna is strongly related to the antenna type and location. Thus, one of the main goals in thermal ablation is the correct antenna placement. The antenna must be placed with high accuracy in the target because a slight deviation could cause damage to the surrounded healthy tissue. Therefore, medical images are used to correctly track the antenna location and insert the antenna at the treatment place.

According to the American Cancer Society, 1720 cases of bone cancer were prognosticated to be deadly in 2020 [12]. Bone tumors are common in long bones, such as the femur and tibia. The most common treatments are surgery (amputation), radiotherapy, and chemotherapy; however, these treatments develop several side effects in patients. Bone tumors are more common in young people; therefore, new treatments to eradicate the tumor and keep the integrity of the healthy bone have been proposed. Microwave ablation (MWA) is considered a minimally invasive technique to generate coagulative necrosis of the tumor cells by increasing their temperature. In clinical practice, thermal ablation for soft tissue has been widely studied, and its biological action mechanisms have been reported [13–17]. Therefore, less information has been reported concerning the thermal ablation for bone tumors. The literature describes several clinical studies to treat bone tumors; however, they were implemented using micro-coaxial antennas to treat soft tissue [10,18–21]. Recently, micro-coaxial antennas designed to treat primarily bone tumors have been studied [10,22–25]. Therefore, new necessities to thoroughly test the antenna's performance have appeared. One of the most important aspects is the antenna location, i.e., it is essential to have a positioning system able to hold and locate the micro-coaxial antenna in the correct place (inside the bone tumor), and the antenna must be located and fixed exactly over the tumor to be treated with microwave thermal ablation.

Despite the evolution and multiple applications of stereotactic systems in neurosurgery, no information about its application in thermal ablation using micro-coaxial antennas has been found. The development of stereotactic systems has been maintained mainly for the skull because it is used mainly for neurosurgery, leaving aside different parts of the body. However, the new applications, such as thermal ablation, required stereotactic systems to treat different locations. In particular, bone cancer is prevalent in large bones; therefore, it is necessary to propose a new system that can easily locate a micro-coaxial antenna over the region to be treated, i.e., adopting the upper or lower limbs shape to place the antenna inside the bone tumor and keep the antenna in the same location during the whole treatment time. In this work, a stereotactic positioning system for thermal ablation of bone tumors is introduced [26]. The design, the materials used for its manufacture, and the construction process of the system are presented. In addition, a series of preliminary tests were carried out to evaluate the accuracy of the displacements made by the stereotactic positioning system [26]. Finally, graphical interface was developed to allow the stereotactic system to be controlled by an external user.

2. Materials and Methods

2.1. Characteristics of the Stereotactic Positioning System to Located Micro-Coaxial Antennas

The stereotactic positioning system developed in this work was designed to locate the antenna around the leg, a region where bone tumors are common. Therefore, the positioning system must hold and move the micro-coaxial antennas such as the ones

described in Figure 1a. These antennas work at 2.45 GHz; they were built in a micro-coaxial cable with outer and inner conductors of 2.19 mm and 0.27 mm, respectively. These antennas have been tested either in phantom or ex-vivo tissue by using 10 W of input power applied per 10 min. Moreover, the standing wave ratio (SWR) of the antennas were from 1.13–1.55, showing a maximum energy transference. Figure 1b shows the axes that must be covered by the displacements of the stereotactic positioning system over the human leg.

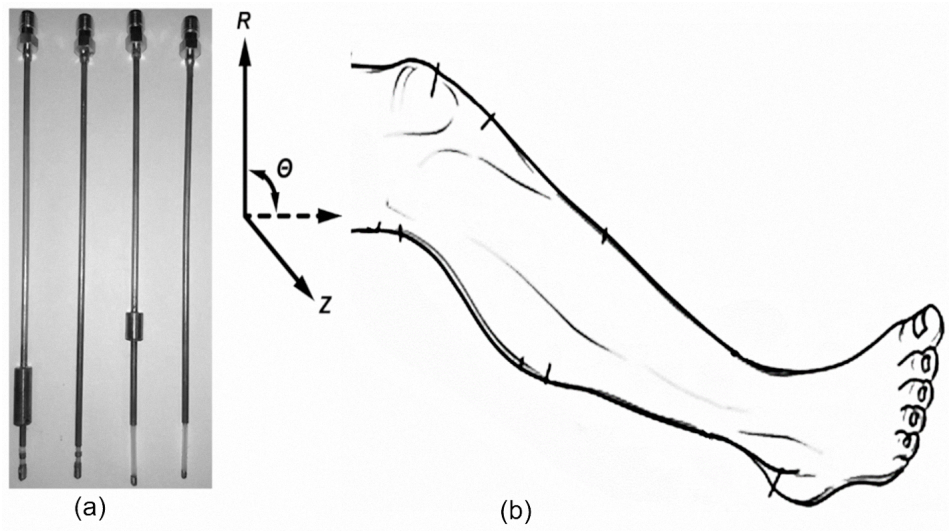

Figure 1. Micro-coaxial antennas and description of the displacements that the stereotactic positioning system must cover. (**a**) Example of four different micro-coaxial antennas designed to treat bone tumors [27], (**b**) axis convention for the stereotactic positioning system (Z-axis, Theta-axis, and R-axis) referred to the human leg.

Because the proposed stereotactic positioning system was designed to be used in a human leg, it was necessary to delimit its dimensions. Therefore, three aspects were considered to delimit the stereotactic positioning system's dimensions:

- User height: It was considered that the length of the leg is linked with the height. The average height of Mexican people was considered, i.e., 1.64 m for men and 1.58 m for women [28]; by considering this information, a length system of 70 cm was proposed (See Figure 2a). Therefore, the Z-axis can be displaced and locate the antenna around that 70 cm mark.
- User weight: The user weight is also a factor to be considered to delimit the dimensions of the stereotactic positioning system. Diseases such as overweight and obesity can cause the leg's subcutaneous adipose tissue to become thicker, affecting its diameter [29]. Therefore, legs with a maximum diameter of 40 cm could be placed; in this case, a maximum antenna length of 17 cm was considered. Figure 2a shows a cylinder (1) representing a transversal view of a human leg placed in the stereotactic positioning system and the direction in which the antenna (2) could be displaced along the Theta-axis.
- Length of the micro-coaxial antennas for thermal ablation: The length of the designed antennas was considered to delimit the stereotactic positioning system's height, Y-axis (See Figure 1a). Although the typical antenna length is 11 cm, future antenna designs could be longer; therefore, 17 cm were chosen as a limit. The final dimensions of the entire system are presented in Figure 2a,b. Figure 2c shows a representation of a human leg in the system and the corresponding axes.

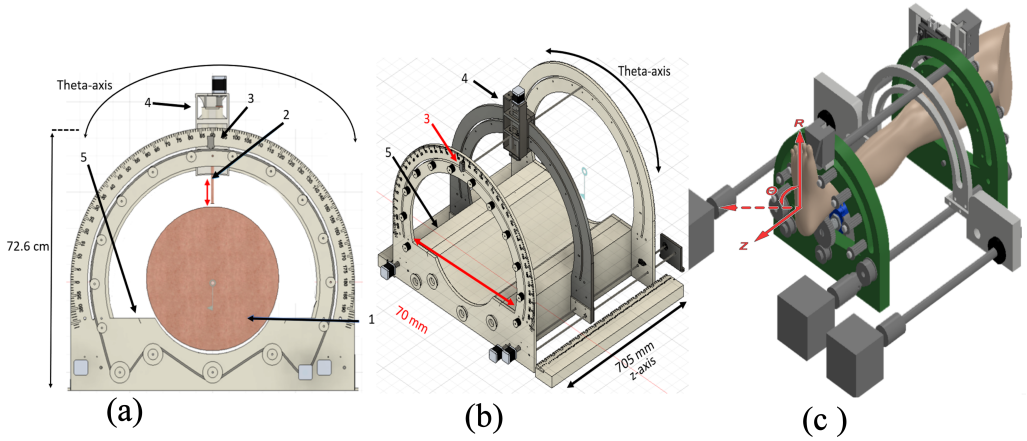

Figure 2. Stereotactic positioning system. (**a**) Front view to show a human leg (1), micro-coaxial antenna (2), visual theta indicator (3), antenna holder (4), and leg support (5); (**b**) isometric view showing the final dimensions of the Z-axis; (**c**) representation of the entire system with the corresponding axes and the leg position.

2.2. Materials Selections

The correct materials to construct a stereotactic positioning system for Microwave Thermal Ablation (MTA) is essential. Two fundamental aspects must be considered for the material selection: the interaction of the material with the electromagnetic field generated by the antennas and the reached therapy temperatures. Ferromagnetic metals placed near the microwave (MW) antenna can modify its radiation pattern [30], and the thermal ablation treatment could be compromised. In order to not modify the antenna radiation pattern, the antenna must not be close to ferromagnetic components. Therefore, selecting a material with a low value (<1) of magnetic permeability is essential. Magnetic permeability is a material characteristic that describes how the material can either generate changes or be affected by electromagnetic fields. Materials with magnetic permeability values over one can distort the antenna electromagnetic field significantly [30]. Moreover, during the treatment, the antenna can generate temperatures between 60 °C and 100 °C [10]; therefore, the selected materials must resist those temperatures.

The materials that satisfy these requirements are acrylonitrile butadiene styrene (ABS), polylactic acid (PLA), and Nylamid XL. The proposed stereotactic positioning system is composed of different pieces; therefore, the materials were selected according to the location of each one. Nylamid XL was proposed to manufacture components that require high mechanical stability, hardness, durability, self-lubrication layer, and resistance to high temperatures, such as the auxiliary stereotactic arc, the stereotactic arc, and the main base. Acrylonitrile butadiene styrene (ABS) and polylactic acid (PLA) were proposed for the manufacture, using 3D printing, of complex parts such as the toothed pulleys. These materials can be used to make pieces outside the antennas' action area because they withstand temperatures below 90 °C. The selected materials can be considered plastics as their magnetic permeability constants are less than 1; due to this characteristic, these materials do not generate alterations to the antennas' electromagnetic field when they are active. Table 1 shows the main features of the selected materials.

Table 1. Advantages and disadvantages of the materials proposed for the construction of the stereotactic positioning system.

Material	Advantages	Disadvantages
Acrylonitrile butadiene	• Resistant to impact • Resistant to high temperatures • Complex parts can be manufactured	Higher temperatures than the ones used for PLA are required to print 3D parts
Polylactic acid (PLA)	• Resistant to impact • Cheap material • Complex parts can be manufactured	If it is exposed to a temperature higher than 90 °C, it could be deformed
Nylamid XL	• High mechanical properties • High terminal resistance • Good machinability • Outer layer to self-lubricant	Parts with high complexity are more difficult to manufacture

2.3. Stereotactic Positioning System

The mechanical design was made by using AUTODESK FUSION 360 software. Although a volume is described in cylindrical coordinates using three axes, the antenna length represents the corresponding R-axis and can be modified by varying the antenna insertion length. Therefore, just the displacements around the areas covered by the Z-axis and Theta-axis were analyzed. In this sense, the stereotactic positioning system can displace and locate the antenna by itself in a specific position.

2.3.1. Z-Axis

The precise movements across the Z-axis were made by stepper motors (NEMA 17). The motor selection took into account the step number and the torque. Nema 17 motor is widely used in applications such as 3D printers, CNC machines, and laser cutters, proving the advantages of this type of motor; technical specifications are 200 steps motor with a step resolution of 1.8° and 3.2 $\frac{kg}{cm}$ torque, which is enough torque for the proposed application—axial anti-backlash nuts were used. Moreover, motors were electromagnetically shielded to reduce the electromagnetic interference due to the field emitted by the motor. The positioning system can achieve an accuracy of 1 mm over the full axis length—70 cm. Figure 3a shows the 3D model of the proposed system and the direction that corresponds to the Z-axis where the antenna can be displaced. On the other hand, the components and parts used to design and assemble a functional stereotactic positioning system that can perform displacements in the Z-axis are presented in Figure 3b.

2.3.2. Theta-Axis

The Theta-axis can also be referred to as an angular position axis; it ranges from 0° to 1800° on a circumference. A minimum displacement of 1° of the system was proposed; further resolution and increasing torque was achieved using a gearbox. Figure 4a shows how the antenna could be displaced across this axis. The movement to perform this displacement is controlled and generated by a stepper motor. However, in this section, conditioning between the toothed pulleys and the toothed belt was implemented. The assembly of the stereotactic positioning system to perform the displacement across the Theta-axis is shown in Figure 4b. The operation principle of this system consists of moving the linear guide in the direction of the theta-axis (See Figure 4b). A stepper motor was coupled to a linear guide that crosses the system along the entire Z-axis to displace across the Theta-axis. A pair of toothed pulleys, fixed by studs, were placed at both extremes of the linear guide. The toothed pulley was placed on the toothed idler rollers of the curved base; moreover, additional tensioners were placed in some positions in the curved base to maintain the proper tension and shape of the toothed band. A clamp coupled to

the toothed belt holds and moves the linear guide over the Theta-axis. Due to the linear guide throughout the system along the Z-axis, it was possible to shift the stepper motor's movement to both sides of the system. On both sides, they have the same configuration for the toothed belt.

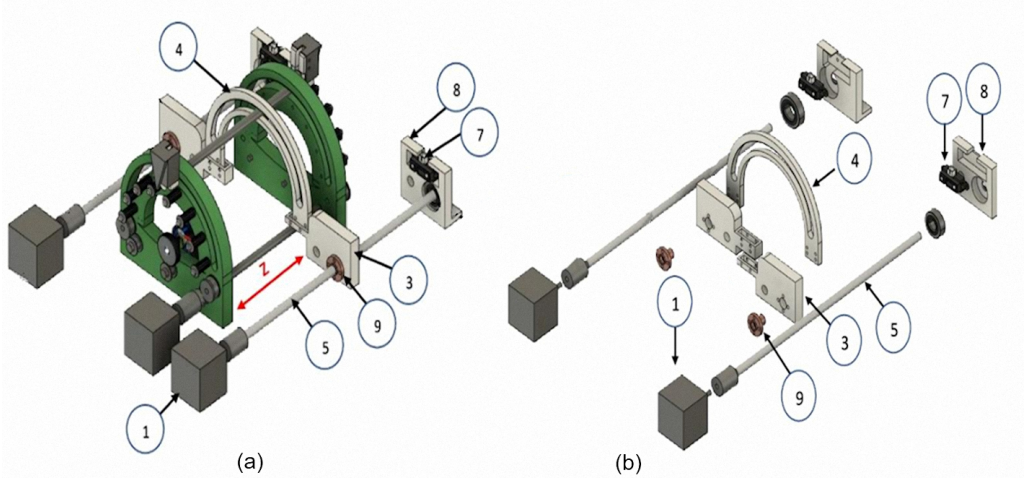

Figure 3. 3D model of the stereotactic positioning system. (**a**) Z-axis and the available length to displace the antenna, (**b**) exploded view of the stereotactic positioning system for displacement in the Z-axis, showing the parts used for the assembly. The stepper motor (1) was coupled one side to the spindle (5), the remaining end was placed in a holder (8), maintaining the line stability and avoiding deformation when the weight is concentrated in some of the ends of the spindle. A piece that will hold the auxiliary stereotactic arc (4) was placed on the spindle, this piece (3) has a space to place a toothed nut (9), and this allows it to move over the length of the spindle. An infrared sensor (7) was placed on the spindle (8) to monitor the displacement in the Z-axis.

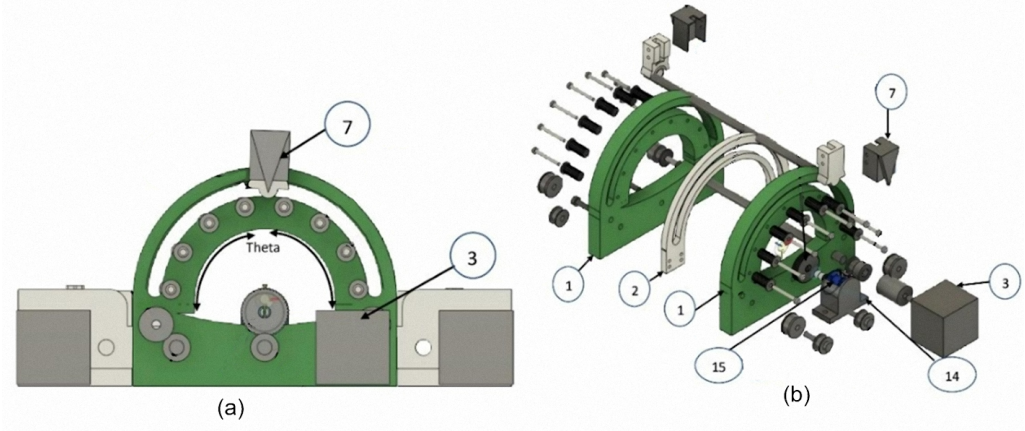

Figure 4. 3D model of the stereotactic positioning system. (**a**) Theta-axis and the available distance to displace the antenna, (**b**) exploded view of the stereotactic positioning system for displacement in the Theta-axis, showing a curved base (1), auxiliary stereotactic arc (2), stepper motor (3), position indicator (7), the base of a potentiometer (14), a precision multiturn potentiometer (15).

2.4. Mechanism Displacements

As previously described, the stereotactic positioning system can perform displacement in two axes (Z and Theta). Figure 1b shows the directions in which the antenna can be displaced. In both cases, the movement was generated by a conditioned system of stepper motors by using toothed belts to move the components. In addition, an electronic driver (Pololu A4899) was configured in a high-resolution mode for both axes (Z and Theta). The motor requires a total of 200 steps to perform a complete revolution; with the driver set

to the high-resolution mode, it was possible to reach $\frac{1}{8}$ step control. Therefore, a total of 800 steps were required to perform one revolution.

2.5. System Characterization

Displacement in the Z-axis was monitored through two infrared sensors (GP2Y0A41SK0F), whereas the Theta axis was monitored using a multiturn precision potentiometer (50 kΩ). Infrared sensors were chosen because they are less sensitive to vibration in this system. The procedure to evaluate the Z-axis displacement was as follows. The system was programmed for moving along the Z-axis in 5 mm steps; the distance was measured using the infrared sensors and compared with the physical displacement measured with a caliper (Scala 222A). This procedure was performed in the available range for measurement on the Z-axis. Finally, the previously obtained values were used to obtain an equation that describes the system's performance in the referred axis. The Theta-axis displacements were evaluated by measuring the Theta-axis angle using a goniometer (Mitutoyo 187-901) and compared with the resistance of a multiturn potentiometer. This measurement protocol was performed 30 times in each axis.

2.6. Graphic Interface

A graphic interface was designed to control the direction and magnitude of the system's displacements in the available axes (Z and Theta). The graphic interface allows us to receive, export, and visualize sensor data to monitor the system position in which the antenna is located. Python version 3.8 was used to develop the graphical interface. Communication between the stereotactic positioning system and the graphic interface was established by using the Arduino DUE board through the StandardFirmata communication protocol. This protocol allows the Arduino DUE board to be used with Python programming. Figure 5 shows the programmatic logic describing the interface function, composed of two classes. The first class controls the current/desired position, and the second class takes control of the data handling, graphical visualization, and whether the data storage is manual or automatic.

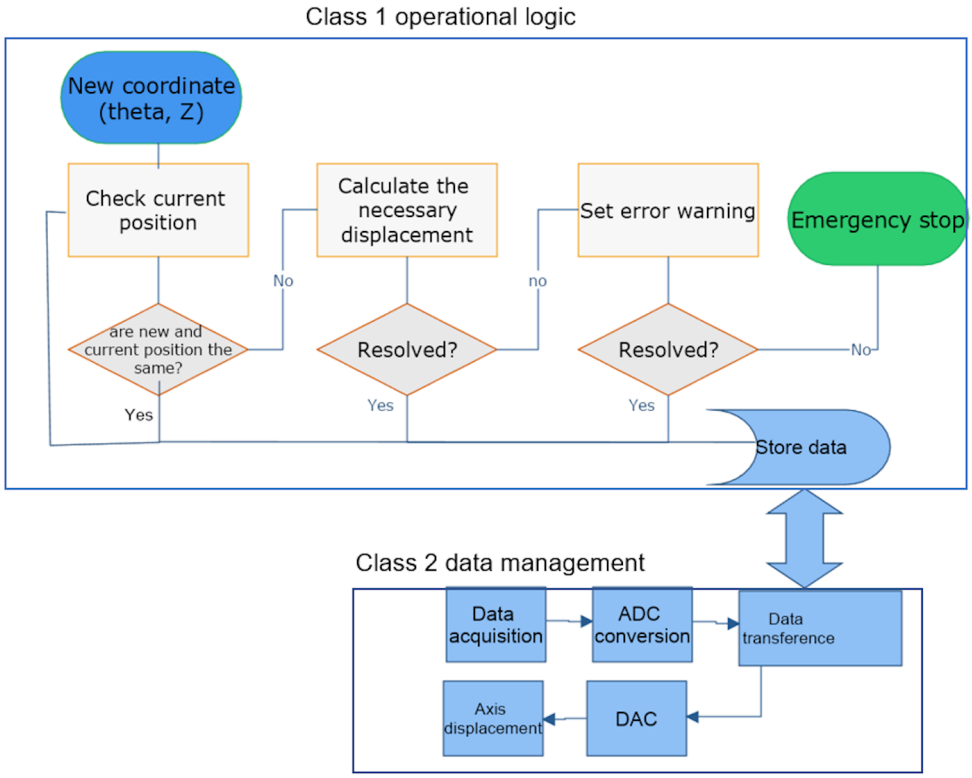

Figure 5. Block diagram of logic use to program the interface.

3. Results

3.1. Stereotactic Positioning System

The stereotactic position system was built using the materials described in Section 2.2 (ABS, PLA, and Nylamid). Figure 6 shows the built system. The parts in green were made using Nylamid due to the forces to which they will be subjected. The arrow in Figure 6a shows one of the motors in charge of moving the system on the Z-axis. It is essential to point out that the motors were covered with diamagnetic material (not shown in the figure) to reduce the possible motor interference in the electromagnetic field generated by the antenna. Tests were performed using a 3D-printed leg model, the size of which considered the Mexican population's average size (360 mm long, ≈172 mm diameter). Regarding electrical power, the entire system is powered by an isolated 12 V direct current power supply. The power supply can be seen in Figure 6b (in blue) and meets the galvanic isolation standards used in medical systems; Figure 6c is an upper view of the developed system. All cables used in the system comply with an electromagnetic shield and the regulations on electrical safety necessary for this type of system.

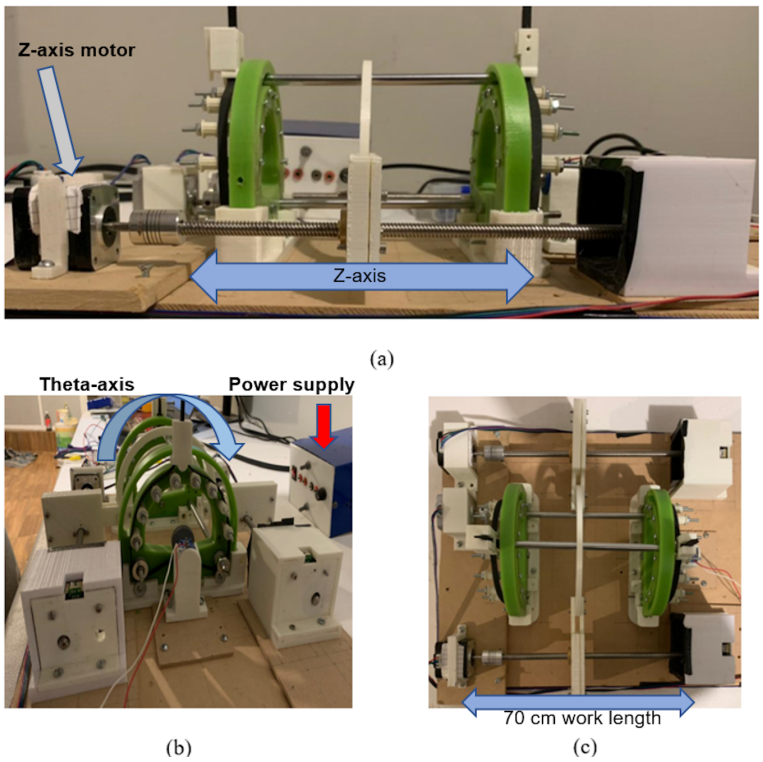

Figure 6. A stereotactic positioning system was constructed showing the (**a**) lateral, (**b**) frontal, and (**c**) superior views.

3.2. Axes Resolution

The Z-axis resolution was enhanced using a transmission and setting the motor driver to a high resolution; therefore, 800 steps are needed to perform an entire revolution; the further resolution is reached using a gearbox (GP42-S1-7-SR) with a reduction ratio of 7:1; therefore, a $\frac{1}{17}^{\circ}$ resolution was achieved. Physical displacement was measured with a caliper, those data were used for modeling the system behavior (See Figure 7). Therefore, the solid line represents the mathematical model (Equation (1)) of the Z-axis displacement as a function of infrared sensor output. The curve of the performance of the Theta-axis is depicted in Figure 8 and the mathematical model is represented by Equation (2). In Equations (1) and (2), I_r and P_r represent the infrared and potentiometer sensors values, respectively

$$Z = -4 + 360e^{-\frac{I_r}{826}} \quad (1)$$

$$Z = -81 + 42e^{\frac{P_r}{40}} \quad (2)$$

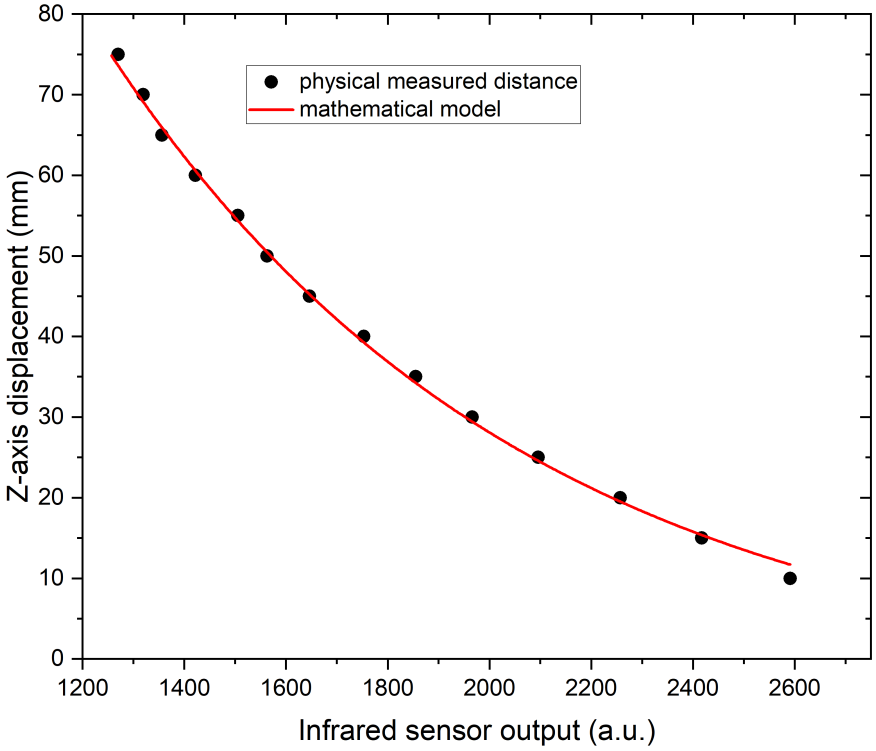

Figure 7. The relationship between the Z-axis displacement and the infrared sensor data: symbols represent the measured physical distances, and the solid line the mathematical model of the Z-axis displacement.

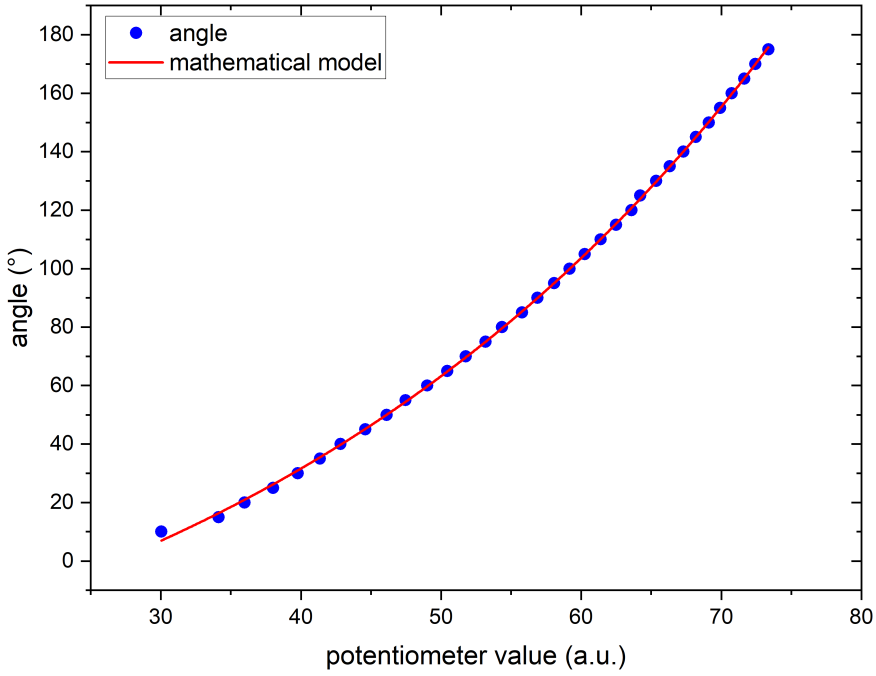

Figure 8. Theta-axis displacement measured with the goniometer as a function of a multiturn potentiometer: the solid line corresponds to a mathematical model obtained from physical displacement.

The accuracy of the displacements generated by the stereotactic positioning system when the user sets a specific value was evaluated. The error between the programmed

displacement and the real one is shown in Figure 9 for the Z-axis. Although the system was designed for a 70 mm traveling distance, the error was determined for the longest possible distance. It was observed that the error is higher at small distances lower than 20 mm; because the infrared sensor is designed for long distances; after 20 mm, the error was lower. On the Z-axis, the results obtained from the infrared sensors show an average error of 0.85 mm. However, it was also observed that there were areas where the sensors did not perform the measurements correctly, affecting the final measurement. These zones appear after the 55 mm distance. The repeatability test reveals an error lower than 1% in the working distance interval for both axes.

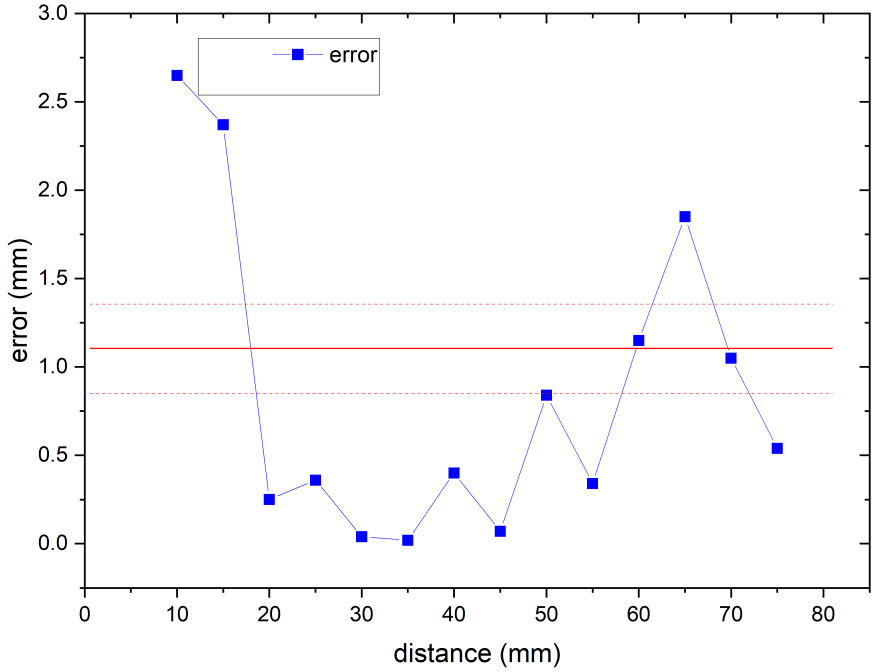

Figure 9. Difference between programmed value and the measured physical value, the red line represents the error mean value and dotted red line the confidence interval.

3.3. Graphic Interface

Figure 10 shows the graphic user interface designed and used to implement the preliminary test. The interface consists of three main sections: Section (1) or the control section. The desired coordinates are introduced using two textboxes provided for the Theta-axis and Z-Axis. Additionally, four buttons were added to implement a manual control; buttons allow displacements from the position to the left and to the right over the Theta-axis and up and down in the Z-axis. Figure 10 shows the graphical user interface developed to manipulate the stereotactic positioning system. Section (2) or the section for displaying the current position. This section shows the values obtained in real-time by the infrared sensors for the Z-axis and the Theta's potentiometer axis. Section (3) or the data export section. The measurements obtained by the three sensors are stored in a table. Once the total measurements were either recorded, or the test was finished, the user can export the data table. The formats in which the table can be exported are .xls and .CSV. This information can be used for further analysis.

The graphical interface allowed the preliminary tests to be carried out in an easier and faster way. First, the graphical interface was able to carry out the movements requested by the user. Furthermore, the interface shows the system's position, providing a way to check the system's accuracy. Finally, the interface is able to store the data obtained by the sensors, export them, and analyze the system's behavior during tests.

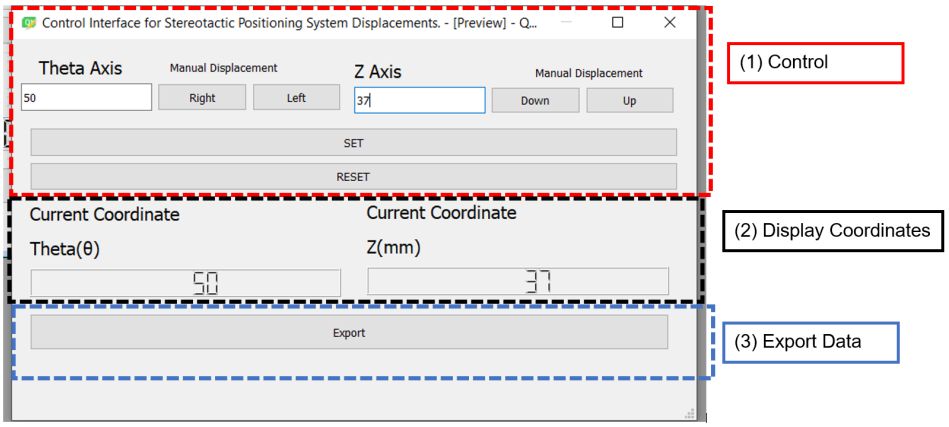

Figure 10. Graphical user interface implemented for preliminary tests of the stereotactic positioning system, showing the sections (1) control displacement, (2) display coordinates, and (3) data export.

4. Discussion

The system was developed with the standard size of the Mexican population; even though no weight morbidities were considered in the design, the system size becomes critical, particularly in the Theta-axis, where obesity can lead to a system limitation. The designed system allows the Theta-axis components to be changed for bigger and smaller sizes; thus, the system can be adapted to overweight people or even children. Despite the advances in computing and manufacturing mechanical components, accuracy is still an issue in stereotactic systems, and the mean accuracy value achieved in this system was 0.85 mm. At the worst conditions, the system can reach an accuracy of 2.5 mm, which is comparable with values reported in the literature for frameless stereotactic systems. Table 2 shows a comparison of the mean accuracy and standard deviation of this system as well as commercial systems, for this comparison to happen, the 3D error was defined as $E = \sqrt{\Delta x^2 + \Delta y^2 + \Delta z^2}$ [31]. It is worth mentioning that, as Bradac and coworkers stated, positioning error in the laboratory conditions is reduced [32]. Although the precision increases for stereotactic systems at laboratory measurements, the values obtained for this system can be compared with those reported in the literature.

Table 2. Mean accuracy comparison with commercial frameless systems.

System	Mean Accuracy (mm)	Standard Deviation (mm)	Theta-Axis Error (°)	Reference
This work	0.85	0.25	2.71	-
Cygnus PFS	1.9	0.7	-	[31]
SMN system	2.61	0.99	-	[31]
ISG viewing	1.67	0.43	-	[31]

The materials used to build the system were chosen to avoid them interfering with the electromagnetic field generated by the ablation antennas. According to preliminary studies, the area covered for the antenna is around 2 cm^2; however, it can reach 10 cm^2 if a multi-array of antennas is used. The system must not interfere with this field; in spite of this, the validation of the effect of the system on the electromagnetic field is necessary. Additionally, it is necessary to work on the system's compatibility with the sterilization processes in the clinic.

5. Conclusions

A stereotactic positioning system to locate microwave thermal ablation antennas over a human leg was developed. The standard size of the Mexican population was used to design the system. The total distance on the Z-axis was 70 cm, which can be considered large enough for most of the Mexican population. On the other hand, a diameter of

40 cm was considered. Infrared sensors were adapted to track and measure the system movements; in the Z-axis working distance, the displacement measured error was 0.85 mm to accurately position microwave antennas for the thermal ablation technique. Moreover, this system allows the operator to either locate or to keep the antenna in the same location during the whole treatment time. The stereotactic system serves for placing micro-coaxial antennas over a human leg, but it can be easily modified to other body parts by adapting the measurements to specific dimensions. It is important to address the fact that the proposed stereotactic positioning system was designed specially to be used as a tool in the thermal ablation therapy. Therefore, all the materials used to build it were chosen in order to reduce as much as possible the interference with the EM energy generated by the micro-coaxial antenna. To our understanding, because the temperature patterns, strongly related to the EM patterns, generated by the micro-coaxial antenna are really focused on the body region ($\approx$2 cm^2) that must be treated, the antenna performance will not be modified by the few metallic components at the stereotactic system. However, to completely validate this information, some experimental tests, considered as a future work, must be done. The next step is a validation of the effect of the system on the electromagnetic field first by numerical simulations and then by measuring the electromagnetic field in conditions similar to the surgery environment. To perform communication between the computer and the stereotactic system, a graphic interface was developed. The interface controls the system's position automatically by using python and StandardFirmata. The interface provides a method to store the system position and sensor data. The repeatability of the positioning system was tested the measured error was lower than 1%, making it comparable to the actual commercial systems.

Author Contributions: Conceptualization, C.J.T.-R. and J.J.A.F.C.; methodology, J.M.M. and G.L.H.; software, J.M.M., C.J.T.-R., G.L.H. and J.J.A.F.C.; validation, J.M.M., C.J.T.-R. and J.J.A.F.C.; formal analysis, C.J.T.-R., A.M.S. and J.J.A.F.C.; investigation, J.M.M. and G.L.H.; resources, C.J.T.-R., A.M.S. and J.J.A.F.C.; data curation, G.L.H. and A.M.S.; writing—original draft preparation, C.J.T.-R. and J.J.A.F.C.; writing—review and editing, J.M.M., C.J.T.-R., G.L.H. and J.J.A.F.C.; supervision, C.J.T.-R. and J.J.A.F.C. All authors have read and agreed to the published version of the manuscript.

Funding: This research received no external funding.

Institutional Review Board Statement: Not applicable.

Informed Consent Statement: This work does not contain any studies with human participants performed by any of the authors.

Data Availability Statement: Data are available from the authors under request.

Acknowledgments: We thank K. Morales Almanza for technical support.

Conflicts of Interest: The authors declare no conflict of interest.

References

1. Renier, C.; Massager, N. Targeting inaccuracy caused by mechanical distortion of the Leksell stereotactic frame during fixation. *J. Appl. Clin. Med. Phys.* **2019**, *20*, 27–36. [CrossRef] [PubMed]
2. Khedr, A.S.; Alaminos-Bouza, A.L.; Brown, R.A. Use of the Brown-Roberts-Wells Stereotactic Frame in a Developing Country. *Cureus* **2018**, *10*, e2126. [CrossRef] [PubMed]
3. Lozano, A.; Gildenberg, P.; Tasker, R. *Textbook of Stereotactic and Functional Neurosurgery*; Springer: Berlin/Heidelberg, Germany, 2009.
4. Trigo Naranjo, J.G.; Anoceto Díaz, J.A. Cirugía estereotáxica en el tratamiento de los tumores cerebrales [Stereotaxic surgery in the treatment of brain tumors]. *Acta Médica Centro* **2014**, *8*, 8.
5. Alptekin, O.; Gubler, F.S.; Ackermans, L.; Kubben, P.L.; Kuijf, M.L.; Kocabicak, E.; Temel, Y. Stereotactic accuracy and frame mounting: A phantom study. *Surg. Neurol. Int.* **2019**, *10*, 67. [CrossRef] [PubMed]
6. Zhang, X.; Zhou, S.; Zhang, Q.; Fu, X.; Wu, Y.; Liu, J.; Liang, B.; Yang, Z.; Wang, X. Stereotactic aspiration for hypertensive intracerebral haemorrhage in a Chinese population: A retrospective cohort study. *Stroke Vasc. Neurol.* **2019**, *4*, 14–21. [CrossRef] [PubMed]
7. Aristu, J.; Ciérvide, R.; Guridi, J.; Moreno, M.; Arbea, L.; Azcona, J.; Ramos, L.; Zubieta, J. Radioterapia estereotáctica [Stereotactic radiotherapy]. *An. Sist. Sanit. Navar.* **2009**, *32*, 61–71. [CrossRef] [PubMed]

8. Madrazo-Navarro, I.; Aldana-Herrero, A. Radiocirugía estereotáctica [Stereotactic radiosurgery]. *CirugíA Cir.* **2005**, *73*, 137–141.
9. Salva Camaño, S.N. Historia de la estereotaxia, la braquiterapia y la radiocirugía en Cuba [History of stereotaxy, brachytherapy and radiosurgery in Cuba]. *Revista Médica Electrónica* **2011**, *33*, 878–892.
10. Trujillo Romero, C.J.; Rico Martinez, G.; Gutierrez Martinez, J. Thermal ablation: An alternative to bone cancer. *Investigación Discapac.* **2018**, *7*, 35–46.
11. Tjong, S. *Advances in Biomedical Sciences and Engineering*; Bentham Science Publishers: Sharjah, United Arab Emirates, 2010.
12. American Cancer Society. Treating Bone Cancer. Available online: https://www.cancer.org/cancer/bone-cancer/treating.html (accessed on 30 May 2022).
13. Karampatzakis, A.; Kühn, S.; Tsanidis, G.; Neufeld, E.; Samaras, T.; Kuster, N. Heating characteristics of antenna arrays used in microwave ablation: A theoretical parametric study. *Comput. Biol. Med.* **2013**, *43*, 1321–1327. [CrossRef] [PubMed]
14. Laeseke, P.F.; Lee, F.T., Jr.; van der Weide, D.W.; Brace, C.L. Multiple-Antenna Microwave Ablation: Spatially Distributing Power Improves Thermal Profiles and Reduces Invasiveness. *J. Interv. Oncol.* **2009**, *2*, 65–72. [PubMed]
15. Taplin, W.; Preston, S.; Varadarajulu, S.; Hancock, C. Comparison of a Loaded Microwave Monopole Antenna and Bipolar RF Electrode Configuration to Assess Variation in Ablation Zone Growth & Visibility under EUS. In Proceedings of the 2019 IEEE Asia-Pacific Microwave Conference (APMC), Singapore, 10–13 December 2019; pp. 1634–1636. [CrossRef]
16. Neagu, V. A study of microwave ablation antenna optimization. In Proceedings of the 2017 E-Health and Bioengineering Conference (EHB), Sinaia, Romania, 22–24 June 2017; pp. 41–44. [CrossRef]
17. American Cancer Society. Técnicas de Cirugía Menos Invasivas para el Cáncer [Less Invasive Surgical Techniques for Cancer]. Available online: https://www.cancer.org/es/tratamiento/tratamientos-y-efectos-secundarios/tipos-de-tratamiento/cirugia/tecnicas-quirurgicas-especiales.html (accessed on 30 May 2022).
18. Simon, C.J.; Dupuy, D.E.; Iannitti, D.A.; Lu, D.S.K.; Yu, N.C.; Aswad, B.I.; Busuttil, R.W.; Lassman, C. Intraoperative Triple Antenna Hepatic Microwave Ablation. *Am. J. Roentgenol.* **2006**, *187*, W333–W340. [CrossRef] [PubMed]
19. Selmi, M.; Iqbal, A.; Smida, A.; Waly, M.I.; Belmabrouk, H. Modeling of heat transfer distribution in tumor breast cancer during microwave ablation therapy. *Microw. Opt. Technol. Lett.* **2022**, *64*, 1364–1375. [CrossRef]
20. Yu, N.C.; Lu, D.S.K.; Raman, S.S.; Dupuy, D.E.; Simon, C.J.; Lassman, C.; Aswad, B.I.; Ianniti, D.; Busuttil, R.W. Hepatocellular Carcinoma: Microwave Ablation with Multiple Straight and Loop Antenna Clusters—Pilot Comparison with Pathologic Findings. *Radiology* **2006**, *239*, 269–275. [CrossRef] [PubMed]
21. Chaichanyut, M. The Modeling Analysis on Porous Media Hepatic Cancer for Microwave Ablation of an Interstitial Helix-Antenna. In Proceedings of the 2018 7th International Conference on Bioinformatics and Biomedical Science, Shenzhen China, 23–25 June 2018; pp. 59–62.
22. Romero, C.J.T.; Martinez, G.R.; Salas, L.L.; Hernandez, A.V.; Martinez, J.G. Micro-Coaxial Slot Antenna to Treat Bone Tumors by Thermal Ablation: Theoretical and Experimental Evaluation. *IEEE Lat. Am. Trans.* **2018**, *16*, 2731–2737. [CrossRef]
23. Ramírez-Guzmán, T.J.; Trujillo-Romero, C.J.; Vera-Hernández, A.; Leija, L. Micro-coaxial Monopole Antenna to Treat Bone Cancer: Design and Preliminary Experimentation. In Proceedings of the 2019 Global Medical Engineering Physics Exchanges/ Pan American Health Care Exchanges (GMEPE/PAHCE), Buenos Aires, Argentina, 26–31 March 2019; pp. 1–6. [CrossRef]
24. Trujillo-Romero, C.J.; Leija-Salas, L.; Vera-Hernández, A.; Rico-Martínez, G.; Gutiérrez-Martínez, J. Double Slot Antenna for Microwave Thermal Ablation to Treat Bone Tumors: Modeling and Experimental Evaluation. *Electronics* **2021**, *10*, 761. [CrossRef]
25. Luján, F.; Pinilla, B.; Gutiérrez-Martínez, J.; Vera-Hernández, A.; Leija, L.; Trujillo-Romero, C.J. Theoretical model of MW antennas to treat bone tumors: One slot and one slot choked antennas. In Proceedings of the 2017 14th International Conference on Electrical Engineering, Computing Science and Automatic Control (CCE), Mexico City, Mexico, 20–22 September 2017; pp. 1–6. [CrossRef]
26. Mendez Maria, J.; Flores Cuautle, J.J.A.; Trujillo-Romero, C.J. Sistema Estereotáctico para Posicionamiento de Antenas de Ablación [Stereotactic System for Positioning Ablation Antennas]. Ph.D. Thesis, Instituto Tecnologico de Orizaba, Orizaba, Mexico, 2021.
27. Ramírez-Guzmán, T.J.; Trujillo-Romero, C.J.; Martínez-Valdez, R.; Leija-Salas, L.; Vera-Hernández, A.; Rico-Martínez, G.; Ortega-Palacios, R.; Gutiérrez-Martínez, J. Thermal Evaluation of a Micro-Coaxial Antenna Set to Treat Bone Tumors: Design, Parametric FEM Modeling and Evaluation in Multilayer Phantom and Ex Vivo Porcine Tissue. *Electronics* **2021**, *10*, 2289. [CrossRef]
28. Medidas Población Mexicana [Mexican Population Measures]. 2021. Available online: https://canaive.mx/descargables (accessed on 30 May 2022).
29. Wallner, S.J.; Luschnigg, N.; Schnedl, W.J.; Lahousen, T.; Sudi, K.; Crailsheim, K.; Möller, R.; Tafeit, E.; Horejsi, R. Body fat distribution of overweight females with a history of weight cycling. *Int. J. Obes.* **2004**, *28*, 1143–1148. [CrossRef] [PubMed]
30. Sadiku, M. *Elements of Electromagnetics*; Oxford University Press: Oxford, UK, 2011.
31. Benardete, E.A.; Leonard, M.A.; Weiner, H.L. Comparison of Frameless Stereotactic Systems: Accuracy, Precision, and Applications. *Neurosurgery* **2001**, *49*, 1409–1416. [CrossRef] [PubMed]
32. Bradac, O.; Steklacova, A.; Nebrenska, K.; Vrana, J.; de Lacy, P.; Benes, V. Accuracy of VarioGuide Frameless Stereotactic System Against Frame-Based Stereotaxy: Prospective, Randomized, Single-Center Study. *World Neurosurg.* **2017**, *104*, 831–840. [CrossRef] [PubMed]